

Original Article

The mTOR-FAK mechanotransduction signaling axis for focal adhesion maturation and cell proliferation

Fan-Yen Lee^{1,9*}, Yen-Yi Zhen^{2*}, Chun-Man Yuen^{3,9}, Raymond Fan⁴, Yen-Ta Chen^{5,9}, Jiunn-Jye Sheu⁴, Yi-Ling Chen², Ching-Jen Wang^{6,9}, Cheuk-Kwan Sun⁷, Hon-Kan Yip^{2,8,9,10,11}

¹Division of Thoracic and Cardiovascular Surgery, Department of Surgery, Kaohsiung Chang Gung Memorial Hospital and Chang Gung University College of Medicine, Kaohsiung 88301, Taiwan; ²Division of Cardiology, Department of Internal Medicine, Kaohsiung Chang Gung Memorial Hospital and Chang Gung University College of Medicine, Kaohsiung 88301, Taiwan; ³Division of Neurosurgery, Department of Surgery, Kaohsiung Chang Gung Memorial Hospital and Chang Gung University College of Medicine, Kaohsiung 88301, Taiwan; ⁴Department of Biochemistry, Hunter College, City University of New York, NY 10065, U.S.A.; ⁵Divisions of Urology, Department of Surgery, Kaohsiung Chang Gung Memorial Hospital and Chang Gung University College of Medicine, Kaohsiung 88301, Taiwan; ⁶Department of Orthopedic Surgery, Kaohsiung Chang Gung Memorial Hospital and Chang Gung University College of Medicine, Kaohsiung 88301, Taiwan; ⁷Department of Emergency Medicine, E-Da Hospital, I-Shou University School of Medicine for International Students, Kaohsiung 82445, Taiwan; ⁸Institute for Translational Research in Biomedicine, Kaohsiung Chang Gung Memorial Hospital, Kaohsiung 83301, Taiwan; ⁹Center for Shockwave Medicine and Tissue Engineering, Kaohsiung Chang Gung Memorial Hospital, Kaohsiung 83301, Taiwan; ¹⁰Department of Medical Research, China Medical University Hospital, China Medical University, Taichung 40402, Taiwan; ¹¹Department of Nursing, Asia University, Taichung 41354, Taiwan, China. *Equal contributors.

Received April 26, 2016; Accepted September 26, 2016; Epub April 15, 2017; Published April 30, 2017

Abstract: Background: Mechanotransduction (MTD) is an important physiopathological signalling pathway associated with cardiovascular disease such as hypertension. Phosphorylation of focal adhesion kinase (FAK) is a MTD-sensing protein. This study tested the hypothesis that mTOR-FAK MTD signaling axis was crucial for focal adhesion (FA) maturation and cell proliferation. Methods: Shock-wave was adopted as a tool for MTD and mTOR-FAK signaling. Results: After demonstrating a failure in FAK phosphorylation after microfilament depolymerization, we attempted to identify the upstream regulator out of three kinases known to be activated in pressure-stimulated MTD [i.e., GSK-3 β , Akt, and mTORC1 (mammalian target of rapamycin complex 1)]. Of the three specific inhibitors, only rapamycin, an inhibitor of mTORC1, was found to inhibit FAK phosphorylation, suggesting that mTORC1 is the upstream regulator in shock-wave-elicited FAK phosphorylation. Moreover, mTOR and its readout protein S6K were found to be activated by shock-wave stimulation. On the other hand, microscopic examination revealed not only MTD-induced increase in the number of actin stress fibers, but also alternative subcellular localization of mTORC1 as vesicle-like inclusions on microfilaments. Besides, rapamycin was found to destruct the granular pattern of mTORC1, while dissociation between F-actin and mTORC1 was noted after cytochalasin D administration. Since mTORC1 and FAK are essential for cell proliferation, we performed proliferation assay for mesenchymal stem cell (MSC) with and without shock-wave administration/rapamycin treatment/FAK depletion. The results demonstrated significant enhancement of cell proliferation after shock-wave stimulation but remarkable suppression after rapamycin and siFAK treatment. Conclusion: Our findings suggest not only a co-ordinated regulation of FAK phosphorylation by mTORC1 and microfilaments, but also the participation of mTORC1-FAK signalling in MSC proliferation.

Keywords: Focal adhesion kinase, shock wave, mammalian target of rapamycin complex 1, cell proliferation

Introduction

Mechanotransduction (MTD) is an important physiological and pathological signalling pathway associated with tissue morphogenesis, and cardiovascular disease such as hyperten-

sion [1, 2]. When a mechanical force imposes on a cell, it passes to inside of the cell and is converted to biochemical signals [3, 4]. Such force stimulation activates mechanosensitive proteins to re-organize cytoskeleton structure and program gene expressions [3, 5-7]. Add-

itionally, cytoskeleton-associated proteins are inevitably required in the regulation of cytoskeletal biological activities [8-10]. Eventually, the mechanical stimuli are extrinsically or intrinsically transformed to cellular processes, such as focal adhesion (FA), cytoskeleton remodeling, force-associated activation of ion channels, cell locomotion and proliferation, and gene expressions [8, 11-13]. The focal adhesion kinase (FAK) in FA complex is a cytoskeleton-associated protein responsible for transducing mechanical stimulations to biochemical processes [14-16]. In response to mechanical stimulation imposed on FA, FAK is phosphorylated [9, 17]. After phosphorylation of FAK at Y576 and Y577 (p-FAK) in its catalytic loop²⁷, this active form of FAK is able to catalyze its substrates [18-20]. In cellular MTD pathway, FAK is one of the pivotal molecules involved in FA complex dynamics that is crucial for modulating cytoskeletal reorganization, regulating cell migration, managing intracellular trafficking, and programming cell proliferation [18, 21-23].

To date, there is no available device that provides well-controlled condition to simulate pressure-induced mechanical force for triggering cellular MTD. It has been reported that shock-wave (SW) stimulation activates cellular MTD through transient pressure [24]. Physically, SW is an acoustic wave that can penetrate and travel through soft tissues [25]. Theoretically, SW creates hydrodynamic pressure through its cavitating effect on aqueous medium [24]. This hydrodynamic pressure creates stress on cells and initiates a cellular MTD process [26-28]. It has been reported that SW-elicited MTD is connected to the suppression of inflammation, activation of cell proliferation, and induction of angiogenesis [29-31]. In this study, SW was used as a device to mimic physiological pressure on cells as an *in vitro* model for studying MTD-elicited subcellular and biochemical changes. Although Akt, mTOR, and GSK-3 β have been reported to be phosphorylated in response to hypertension in clinical cases and *in vivo* studies [32-38], such as elevated blood pressure on the vascular wall in hypertension [36, 39, 40], the relationships among Akt, mTOR, GSK-3 β , and FAK in MTD remain unclear. Additionally, kinases are known to be upregulated in hypertension and proposed as disease

markers [41, 42]. Accordingly, pharmacological blocking was adopted in the present study to screen for the upstream kinase(s) responsible for SW-induced FAK activation. The results were reflected in the ratio of p-FAK/FAK after blockade of a specific kinase.

Materials and methods

Shock-wave treatment

In this study, the SW machine was designed and produced by Eva trode (Swiss), and the type of SW probe applied in SW treatment was RE005 with energy flux density (EFD) range from 0.10 to 0.15 mJ/mm². The SW traveled through a plastic cover and 2 cm PBS layer to the cells layer. Each treatment comprised 100 impulses. Prior to the SW treatment, 5 \times 10⁵ cells were seeded on 100 mm Petri dish or 10⁴ cells were seeded on 18 mm diameter round coverslip in a 12-well plate and allowed to grow for 48 hours. Twelve hours after SW treatment, the cells were harvested and cell lysates were subjected to either Western blot analysis or immunofluorescent staining.

Immunofluorescent staining and immunofluorescent microscopic imager

The Olympus Bx-51 epifluorescence microscope (Olympus, Kyoto, Japan) equipped with X-Cite 120PC microscope laminators (Excelitas Technologies, Wiesbaden, Germany), and dual DP70 digital camera (Olympus, Kyoto, Japan) was used to observe and capture fluorescent signals. The cells were seeded on 18 mm coverslip in 12 well culture plate. Examining SW caused cell damage, the cells on coverslip subjected to shockwave treatment were immediately fixed in 4% paraformaldehyde in CSK buffer (10 mM Pipes, 100 mM NaCl, 3 mM MgCl₂, 1 mM EGTA, 300 mM sucrose, pH 6.8) for 10 minutes, and permeabilized in 0.5% Triton in CSK buffer for 5 minutes. Investigating FAK associated signaling, the cells were fixed after 12 h SW application. The antibodies used were as follows: β -tubulin (1:500, Abcam), FAK (1:500, Santa Cruz Biotechnology), p-FAK (p-FAK-Y576/577) (1:300, Cell signaling), mTORC1 (1:300, Cell Signaling), p-mTORC1 (Ser2448) (1:200, Cell Signaling), α -actinin (1:500, Santa Cruz Biotechnology), Paxillin (1:500, Santa Cruz Biotechnology), and p-Paxillin (1:300, Santa

mTOR-FAK axis and cell proliferation

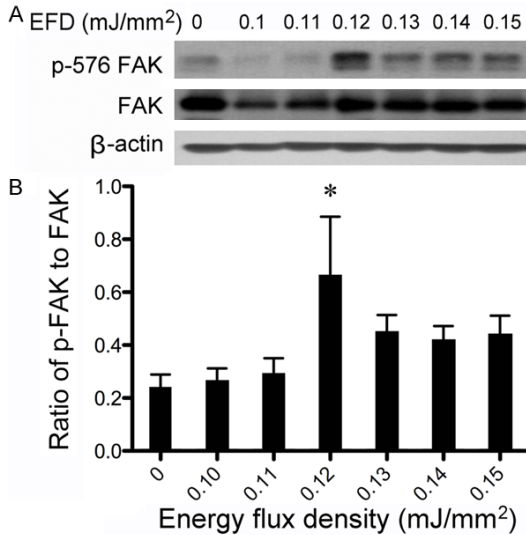


Figure 1. Verification of optimal shock-wave dosage for FAK phosphorylation (p-FAK) in rat mesenchymal stem cells (MSC). A. Identification of an optimal energy flux density (EFD) of 0.12 mJ/mm² for p-FAK through Western blot analysis. B. Statistical analysis, showing maximal p-FAK/FAK at a shock-wave EFD of 0.12 mJ/mm². *P<0.01 vs. other groups.

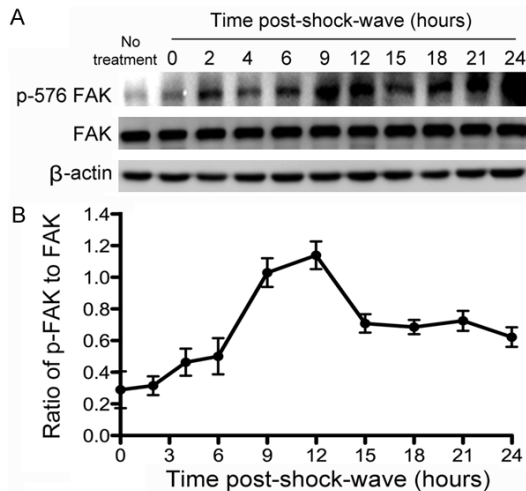


Figure 2. Identification of the optimal duration of shock-wave stimulation for maximal P-FAK in rat MSC with an EFD of 0.12 mJ/mm². A. Ratio of phosphorylated FAK (p-FAK) to FAK highest at post-shock-wave 9 h and 12 h. B. Statistical analysis on the ratio of p-FAK to FAK showing a quasi-parabolic change with peak value noted at 12 h after shock-wave treatment.

Cruz Biotechnology). Additional reagents used were TRITC/FITC phalloidin (1:1000; Sigma-Aldrich), and DAPI (1:500, Sigma-Aldrich). Cells nuclei were stained with 0.2 µg/mL 4',6-diamidino-2-phenylindole (DAPI; Sigma).

The p-FAK-Y576/Y577 stained focal adhesion size quantification

The MSC were fixed with 4% PFA and 0.5% Triton x-100 for 20 minutes, and immunofluorescently stained with antibody against p-FAK-Y576/Y577 epitope and TRITC conjugated phalloidin to defined focal adhesion at tip of actin stress fibers. Cells were imaged with Olympus Planapo 60x/1.40 ∞ /0.17 Oil Microscope Objective (Olympus, Kyoto, Japan) and pictures were captured with an automated microscope stage and digital image acquisition driven by custom program cellSens software (Olympus, Japan). The areas of p-FAK-Y576/Y577 stained focal adhesion was marked by free-hand-polygon a mask with the p-FAK antibody signal tagged with Alexa 488 at tip of TRITC-phalloidin stained F-actin stress fibers and high-resolution digital images analyzed by the cellSens Digital imaging software (Olympus, Japan).

FAK knockdown

FAK protein depletion in MSC was performed with the oligonucleotide transfection. The oligonucleotides were designed (5'-UCUCCAUGCCUGAUAUACUGGCCdtdt-3', and 5'-GGGCCAGUAUUAUCAGGCAUGGAGAdtdt-3') matched to rat FAK mRNA (Sigma). 2×10^5 cells were cultured in 35 mm Petri dish for 24 hours before transfection. For the FAK knockdown, the oligonucleotides transfection into MSC was carried out with liposfetamin transfection according to the manufacture's manual (Invitrogen). As controls, oligonucleotides with a similar length but irrelevant sequence purchased from sigma. For the negative control siRNA, the non-Targeting siRNA, contains at least four mismatches to any human, mouse, or rat gene, was previously determined by the manufacture using Microarray. This scrambled sequence is 5'UAAGGCUAUGAAGAGAUAC-3' (Sigma). At post-transfection 48 h, 72 h, 96 h, the cells were harvested and cells lysates were subjected to Western analysis, respectively.

Statistical analyses

Quantitative data are expressed as means \pm SD. Statistical analyses were performed by ANOVA, followed by Bonferroni multiple-comparison post hoc test. SAS statistical software for Windows version 8.2 (SAS institute, Cary, NC) was utilized. A P value of less than 0.05 was considered statistically significant.

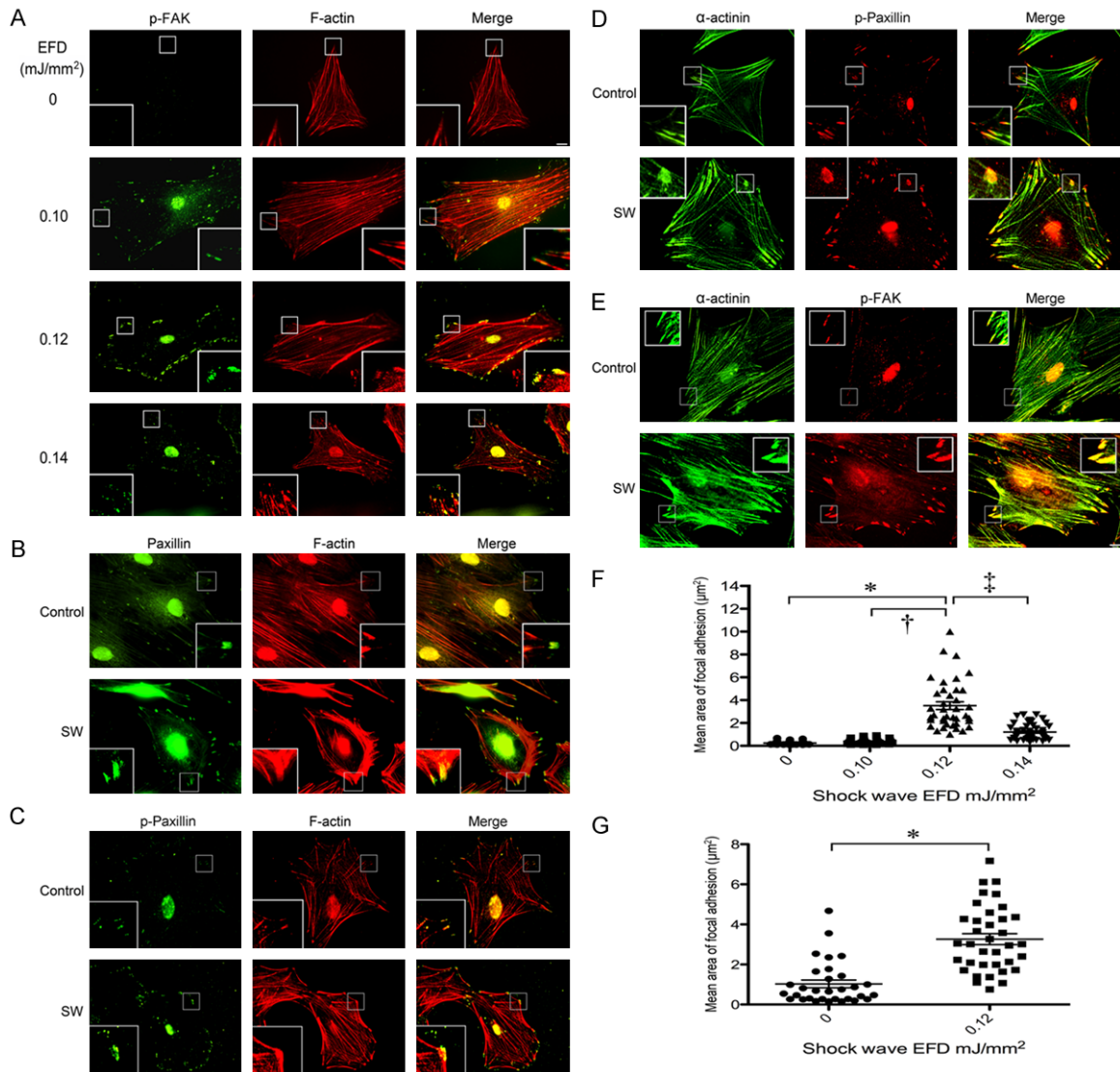


Figure 3. Immunofluorescent microscopic identification of focal adhesion (FA) complex in rat MSC following treatment with shock-wave (SW) of different energies. A. Staining with antibodies against phosphorylated FAK (p-FAK) (green) and phalloidin for F-actin (red), illustrating progressive increase in p-FAK translocation to cell membrane as SW energy increased from an EFD of 0 to 0.12 mJ/mm², but substantial reduction noted after treatment with energy of 0.14 mJ/mm². B. Magnification of FA shown at the corner of each figure. Enlargement of paxillin representing FA remodelling after SW treatment. Paxillin phosphorylation at tyrosine 31 in focal contact after 0.12 mJ/mm² shock wave application. C. The presence of the p-paxillin in FA colocalizes with α -actinin. Translocation of α -actinin from stress fibers (Control) to FA after SW treatment, indicating adhesion maturation. D. SW-enriched p-FAK presentation in FA complex compared to barely identifiable p-FAK in the controls. E. Co-localization of α -actinin and p-FAK in merged image after SW treatment, suggesting the formation of complex from the two proteins. F. Quantification of FA areas with p-FAK following stimulation with different SW energies. * $P < 0.0001$ vs. 0 mJ/mm²; † $P < 0.0001$ vs. 0.1 mJ/mm²; ‡ $P < 0.0001$ vs. 0.14 mJ/mm². G. Quantification of FA areas with p-Paxillin following stimulation with SW at an EFD of 0.12 mJ/mm². * $P < 0.0001$ vs. 0 mJ/mm². Scale bars represent 20 μ m.

Results

Effects of SW energy flux density (EFD) of 0.12 mJ/mm² on FAK phosphorylation at Y576/Y577

Adipose-derived MSC isolated from the adipose tissue surrounding the epididymis of adult

male Sprague-Dawley (SD) rats were cultured in low-glucose DMEM medium to metabolically exclude adipocytes and fibroblasts from mesenchymal stem cell (MSC) population ([Supplementary Figure 1](#)). Besides, the phenotype of MSC population was confirmed by the positivity of CD29, CD90, and CD105 and negativity

mTOR-FAK axis and cell proliferation

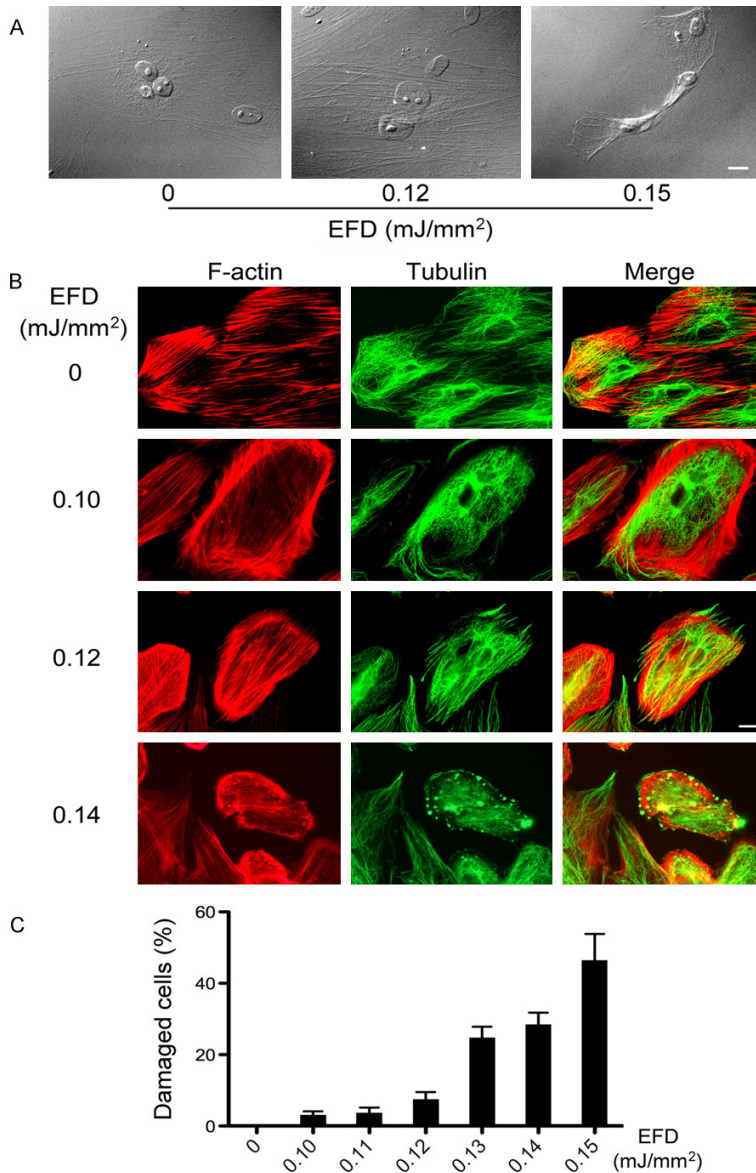


Figure 4. Examination of SW-induced damage in rat MSC. A. Nomarski microscopy examination showing absence of cellular structural damage following SW treatment with an EFD of 0.12 mJ/mm². Cellular damage evident after treatment with SW of EFD 0.15 mJ/mm², as reflected in nuclear round-up, nuclear shrinkage and conspicuous rounding up of the treated cells, respectively. B. Immunofluorescent staining with TRITC-conjugated phalloidin and anti- β -tubulin for staining of F-actin (red) and microtubule green), respectively, showing absence of notable changes in cytoskeleton after SW treatment of EFD up to 0.12 mJ/mm². Marked cytoskeletal damage presenting as debris of filamentous actin and microtubules (i.e., fluorescent granules) peripherally distributed because of their attachment to cell membrane after SW treatment with an EFD of 0.14 mJ/mm². C. Analytical results of the number of cell damage, $P < 0.0001$ on ANOVA analysis. Scale bars represent 20 μ m.

of CD34 and CD45 through flow cytometric analysis to exclude hematopoietic cell contamination (Supplementary Figure 1).

Prior to SW treatment, the cells were seeded on a 100 mm Petri dish or 18 mm diameter cover-

slip for 48 hours to avoid SW-elicited detachment of cells from the Petri dish. The application of SW on adherent MSC is depicted schematically in Supplementary Figure 1. The SW travels through PBS layer to reach the MSC (Supplementary Figure 1).

Firstly, to determine the optimal energy flux density (EFD) of SW for maximizing FAK phosphorylation at Y576 and Y577, EFD starting from 0.10 mJ/mm² with progressive increment of 0.01 mJ/mm² to 0.15 mJ/mm² were applied to MSC growing on 100 mm Petri dish (Supplementary Figure 1). Twelve hours after SW treatment, the cells were harvested and the cell lysate was subjected to Western blotting analysis. The Western blot data from six independent experiments were statistically analyzed to obtain a stoichiometric ratio of phosphorylated FAK to non-phosphorylated FAK (i.e., p-FAK/FAK ratio) (Figure 1A) that was found to be slightly increased on elevating EFD from 0.10 to 0.12 mJ/mm². Statistical analysis demonstrated a p-FAK/FAK ratio close to 0.7 in 0.12 mJ/mm² SW treated cells, whereas the ratio was approximately 0.25 and 0.40 for 0-0.11 mJ/mm² and 0.13-0.15 mJ/mm², respectively. The results demonstrate that FAK phosphorylation is not energy-dependent (Figure 1B), suggesting that SW of EFD 0.12 mJ/mm² is optimal for maximizing FAK phosphorylation in MSC.

Changes in the ratio of p-FAK/FAK in MSC at different time points following SW stimulation at an EFD of 0.12 mJ/mm² were relatively quantified by Western blot (Figure 2A). While the p-FAK/FAK ratio in MSC without SW treatment was below 0.2, the ratio was slightly increased

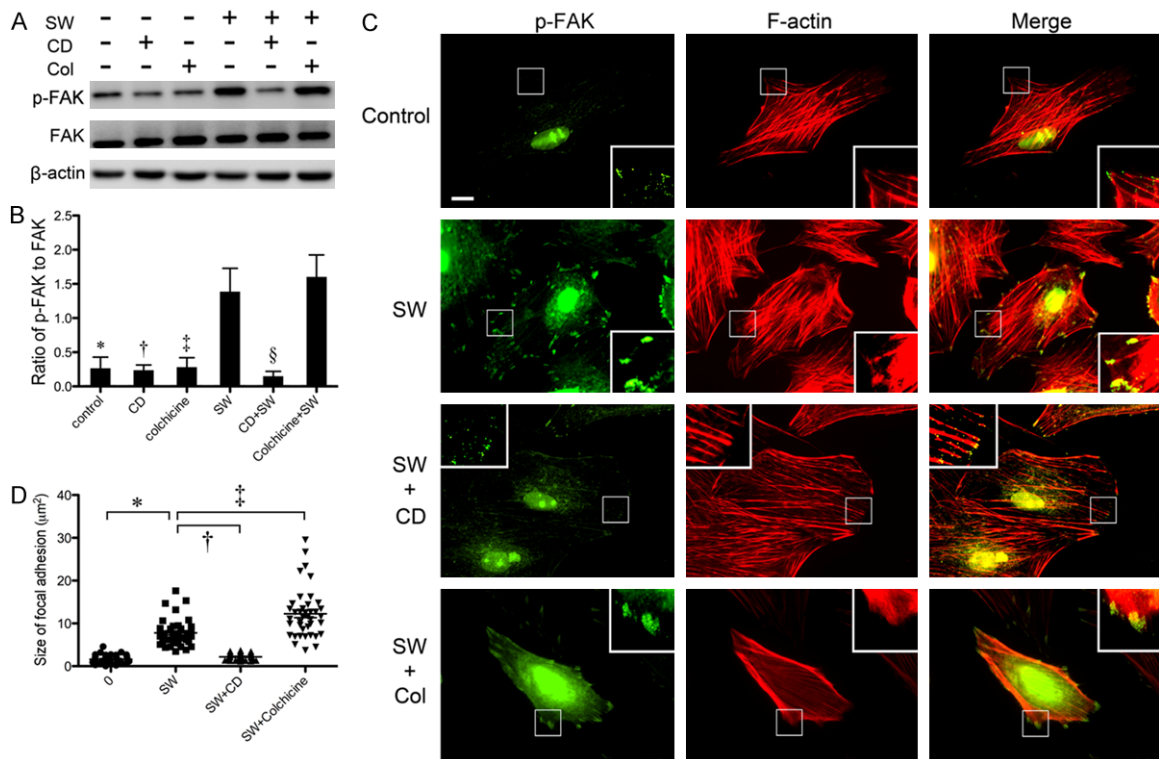


Figure 5. Effects of microfilament and microtubule depolymerization on p-FAK in rat MSC. **A.** Western blot analysis of p-FAK of rat MSC after pretreatment with either cytochalasin D (CD) or colchicine (Col) for 2 hours before treatment with SW of energy 0.12 mJ/mm², showing substantial enhancement of P-FAK after SW stimulation but remarkably interrupted after CD pretreatment. **B.** Statistical analysis on the ratio of p-FAK to FAK demonstrating consistent results. With respect to SW: *P = 0.0195 vs. 0 mJ/mm²; †P = 0.0228 vs. CD; ‡P < 0.05 vs. Col; §P = 0.024 vs. SW + CD; P = 0.06 vs. SW + Col. **C.** Immunofluorescent microscopic examination of plasma membrane translocation of p-FAK (green) to tip of F-actin (red) with either CD or Col pretreatment before SW stimulation, highlighting (small squares) the enhancement of P-FAK after SW treatment but inhibited by CD pretreatment. Inhibition not noted after Col pretreatment. **D.** Statistical analysis of FA areas with either CD or Col pretreatment before SW stimulation. With respect to SW: *P < 0.0001 vs. 0 mJ/mm²; †P < 0.0001 vs. 0.1 mJ/mm²; ‡P < 0.0001 vs. 0.14 mJ/mm².

to 0.5 from 0 h to 6 h following SW treatment. The ratio then showed a steep elevation between post-SW 6 h and 9 h from 0.6 to 1.0 and persistently increased till post-SW 12 h when the highest ratio 1.2 was reached. On the other hand, the ratio dropped drastically to 0.6 fifteen hours after cessation of SW stimulation till the end of 24 hours after initial SW administration (Figure 2B).

SW induces FAK translocation to focal adhesions

To trace alternative subcellular localization of FAK after 12 h post SW stimulation, antibodies recognizing FAK as well as phosphorylated Y576 and Y577 in FAK were applied in fluorescent imaging study (Figure 3A). The results demonstrated immunofluorescent staining (i.e., FAK phosphorylation) at the tips of actin stress

fibers which are the positions of focal adhesions following SW administration with the optimal EFD of 0.12 mJ/mm² (Figure 3A).

Plotting the average p-FAK-based focal adhesion size against SW energy of 0, 0.10, 0.12, and 0.14 mJ/mm² demonstrated a mean area of approximately 0.5, 0.5, 4 μm², and 1 μm², respectively (Figure 3F). The results are consistent with those from Western blotting that also identified an EFD of 0.12 mJ/mm² as the optimal energy level for inducing the maximal p-FAK/FAK ratio of 0.7 and also the largest mean p-FAK-based focal adhesion size of 4 μm² (Figures 1A, 3A, 3F).

SW enhanced tyrosine 31 phosphorylation of paxillin

To corroborate enzymatic function of FAK in phosphorylating paxillin at focal adhesions,

mTOR-FAK axis and cell proliferation

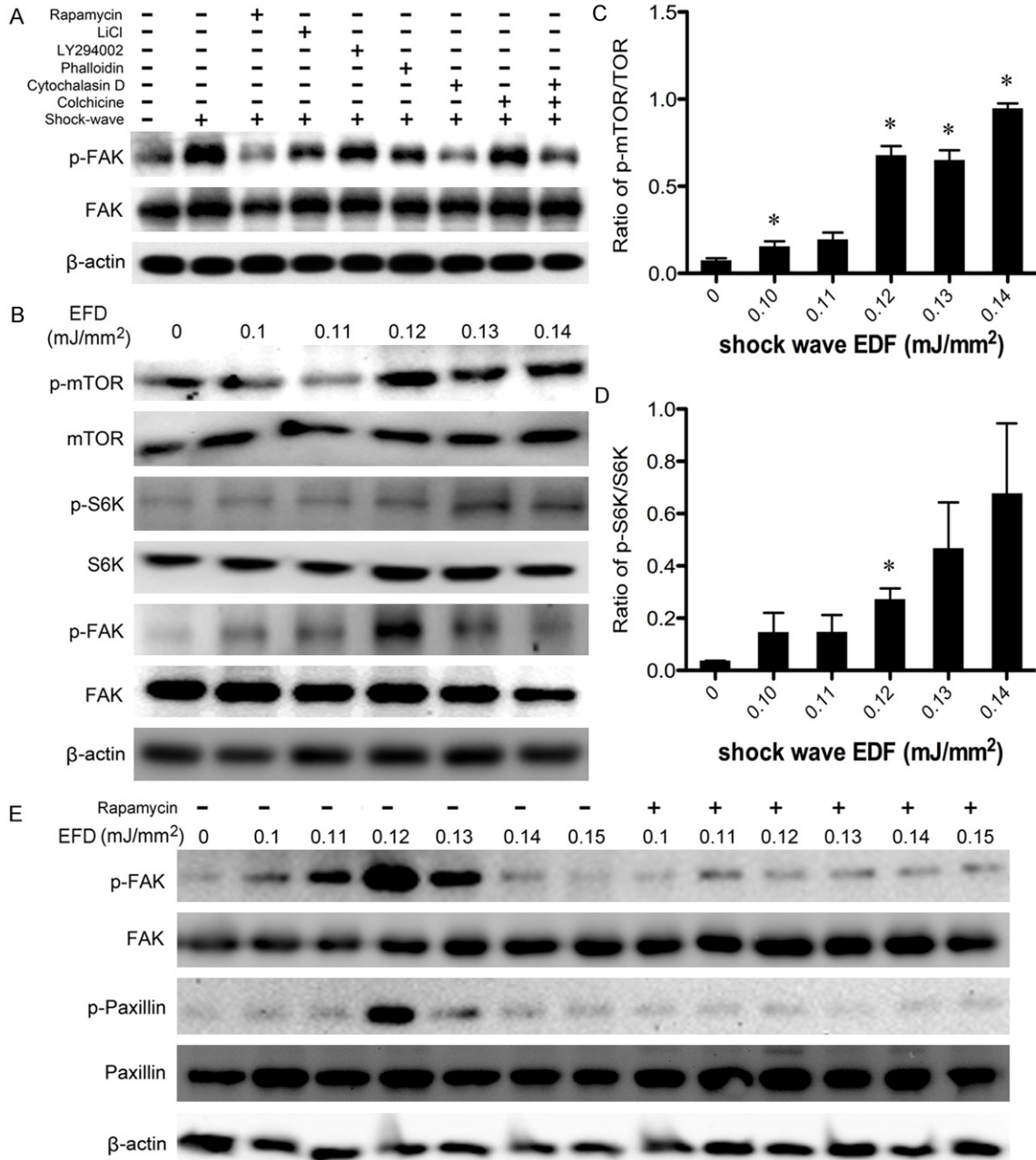


Figure 6. Role of mTORC1 and F-actin in p-FAK in rat MSC. A. Inhibition of GSK-3 β , Akt, and mTORC1 with lithium chloride, LY294002, and rapamycin, respectively, in rat MSC before SW stimulation (0.12 mJ/mm²). Note the remarkable interruption of p-FAK after rapamycin pretreatment and substantial enhancement of p-FAK expression after SW stimulation. B. Progressive elevation in phosphorylation at S2448 of mTOR (p-mTOR) on increasing EFD of shock-wave from 0 to 0.14 mJ/mm². Similar elevations noted in phosphorylation of S6K at T389 (mTOR activation readout protein) on increasing SW energy. Significantly enhanced FAK phosphorylation only after SW stimulation at an energy level of 0.12 mJ/mm². C. Quantification of protein expression of p-mTOR on increasing SW energy. D. Quantification of protein expression of phosphorylated p70 ribosomal S6 kinase (p-S6K) on increasing SW energy from results of western blotting. *P<0.05 vs. SW energy 0 mJ/mm². E. Demonstration of p-FAK and its substrate, paxillin, by SW stimulation at different energy levels which was abolished after rapamycin treatment. Note highest p-FAK and p-paxillin levels after SW stimulation at an EFD of 0.12 mJ/mm².

Western blot and immunostaining with antibody specifically recognizing p-Y31 paxillin were

carried out with or without SW stimulation. The results showed that, although there was no sig-

mTOR-FAK axis and cell proliferation

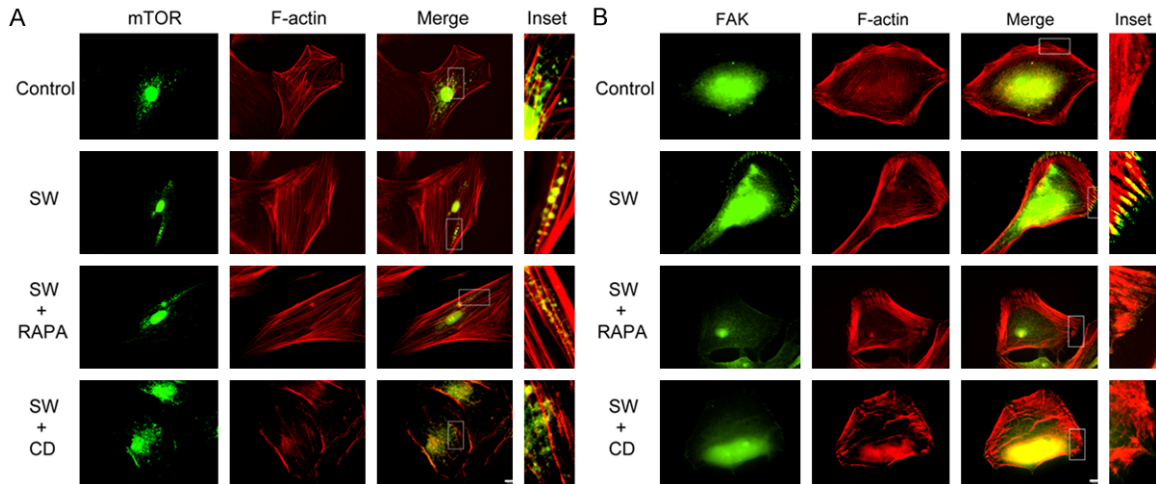


Figure 7. Effects of SW on mTOR and p-FAK subcellular distribution in rat MSC. A. Note the random punctate distribution of mTOR (green) around nucleus without SW stimulation (control) compared with vesicle-like inclusions associated with actin stress fibers (red) after SW application. Diminished punctuated pattern of mTOR associated with actin stress fibers in MSC with rapamycin pre-treatment for mTORC1inhibition before SW treatment. Peri-nuclear punctuated pattern of mTOR with dissociation from actin stress fibers after actin depolymerization with cytochalasin D before SW stimulation. B. Absence of plasma membrane translocation of FAK (green) without SW stimulation compared to membrane localization of FAK associated with actin stress fibers (red) after SW treatment. Neither FAK translocation nor its association with actin stress fibers noted after pre-treatment with rapamycin or cytochalasin D before SW stimulation.

nificant change in paxillin expression (**Figure 3B**), phosphorylation of paxillin was notably increased from $0.5 \mu\text{m}^2$ to $5 \mu\text{m}^2$ after SW stimulation (**Figure 3C, 3G**). Consistent elevation in p-paxillin expression was noted in Western blotting after SW stimulation at an EFD of $0.12 \text{ mJ}/\text{mm}^2$ (**Figure 6E**).

SW induces focal adhesion maturation and α -actinin redistribution to focal adhesions

To confirm SW-activated focal adhesion maturation, antibodies against p-FAK, p-paxillin, and α -actinin were employed in immunostaining that demonstrated colocalization of p-paxillin and α -actinin (**Figure 3D**) and that of p-FAK and α -actinin (**Figure 3E**) at focal adhesions after SW stimulation at an EFD of $0.12 \text{ mJ}/\text{mm}^2$.

SW of EFD higher than $0.12 \text{ mJ}/\text{mm}^2$ causes cytoskeletal damage

To investigate the phenomenon from a morphological point of view, we found that while cell morphology is mostly preserved on Nomaski contrast interference microscopy when MSC are subjected to SW stimulation of EFD $0.12 \text{ mJ}/\text{mm}^2$, cell deformity becomes evident following SW administration of EFD over $0.13 \text{ mJ}/\text{mm}^2$.

mm^2 and remarkable deformation is noted (e.g. cellular round-up) after application of SW of EFD $0.14 \text{ mJ}/\text{mm}^2$ (**Figure 4A**).

When the force of SW is over the mechanical strength of cytoskeletons (i.e., EFD = $0.13 \text{ mJ}/\text{mm}^2$), distorted cytoskeletal structure with altered cell shape is noted (**Figure 4B**). When SW of EFD $0.10 \text{ mJ}/\text{mm}^2$ was applied on the cells, the microtubules lost its astral organization (**Figure 4B**). Severe cytoskeletal destruction in MSC became apparent when SW of EFD $0.14 \text{ mJ}/\text{mm}^2$ or higher was imposed on the cells. The results, therefore, suggest that the mechanical strength of microfilaments and microtubules can withstand a SW of EFD approximately $0.12 \text{ mJ}/\text{mm}^2$.

When SW of EFD $0.13 \text{ mJ}/\text{mm}^2$ was applied to the MSC, shrinkage of cells from destruction of peripheral microfilaments and microtubules was evident on phase contrast microscopy (**Figure 4B**). On immunofluorescent examination, damaged microfilaments presented as phalloidin-positive F-actin debris in the peripheral region of the cells, instead of depolymerized G-actin that cannot be stained by phalloidin (**Figure 4B**). When SW of intensity over 0.12

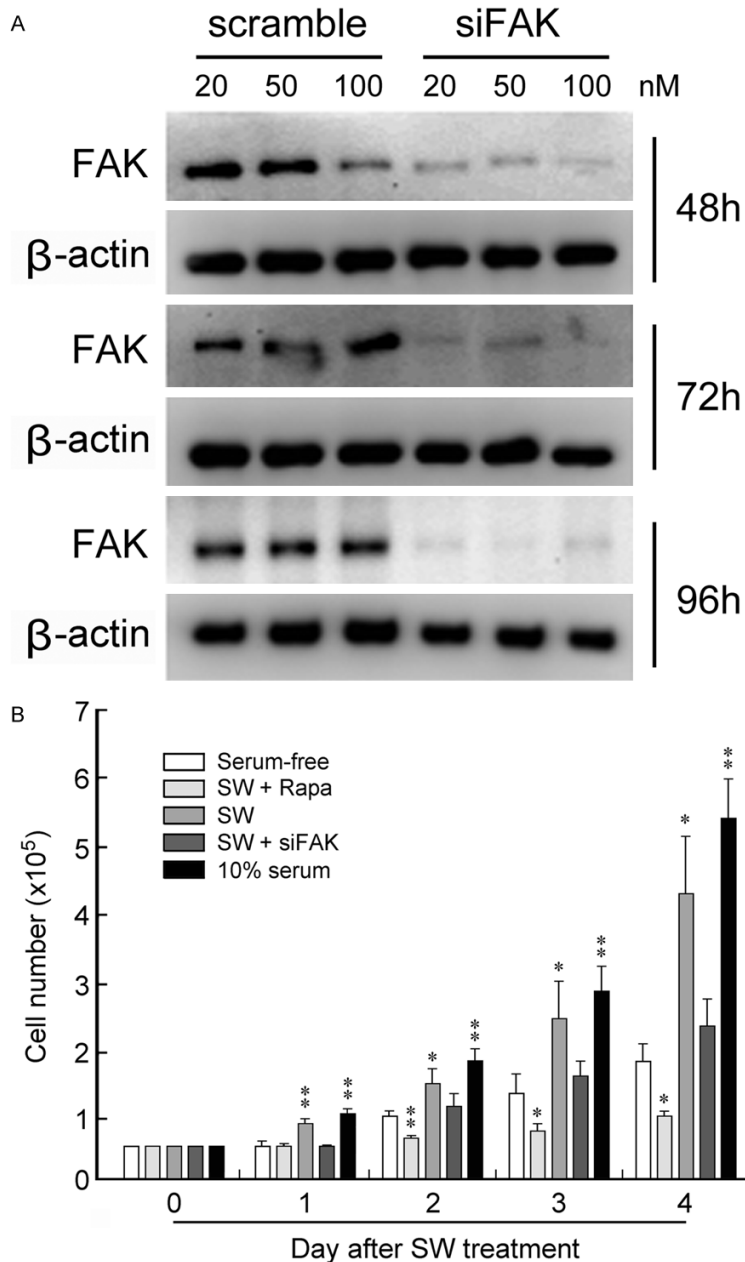


Figure 8. FAK depletion using siFAK and the effects of SW, FAK depletion, and mTOR inhibition on proliferation of rat MSC. A. FAK depletion using different concentrations (i.e., 20, 50, and 100 nM) of siFAK after 48, 72, and 96 hours of treatment, showing substantial suppression of FAK protein expression compared with non-targeting oligo-nucleotides (scramble). B. Note significant suppression of cell proliferation after rapamycin (Rapa) treatment and abolishment of SW-elicited cell proliferative effect after FAK depletion with siFAK. *P<0.05 vs. Serum-free group, **P<0.005 vs. Serum-free group.

mJ/mm² was applied (i.e., 0.13 mJ/mm²), there was a substantial increase in the number of damaged cells which was as high as 50% after treatment with SW of EFD 0.15 mJ/mm² (Figure 4C).

mTORC1 is an upstream kinase regulating FAK phosphorylation after SW triggered MTD

We test the hypotheses that (1) SW creates a hydrodynamic effect on MSC equivalent to that

Microfilaments, but not microtubules, play an important role in FAK activation

To elucidate the two possible causes that hamper FAK phosphorylation, namely, depolymerization of microfilament and/or microtubules, chemical depolymerization was performed by pre-treating MSC with cytochalasin D (i.e., an actin-depolymerizing factor) and colchicine (i.e., a microtubule-perturbing agent) for 2 hours before treatment with SW of EFD 0.12 mJ/mm². Western blot analysis on the p-FAK/FAK ratio showed that, while the administration of colchicine did not interrupt FAK phosphorylation, pre-treatment with cytochalasin D substantially diminished FAK phosphorylation (P<0.05) (Figure 5A, 5B). This finding, therefore, highlights the important role of microfilaments, but not microtubules, in SW-induced MTD for FAK phosphorylation (Figure 5B). Consistently, immunofluorescent study on phosphorylated FAK showed that pre-treatment with colchicine has no significant impact both on FAK phosphorylation level and FAK translocation at focal adhesion compared with the positive controls (Figure 5C). Statistical analysis of focal adhesion areas with cytochalasin D and colchicine pretreatment before SW stimulation showed highly significant reduction in the former but substantial elevation in the latter (Figure 5D).

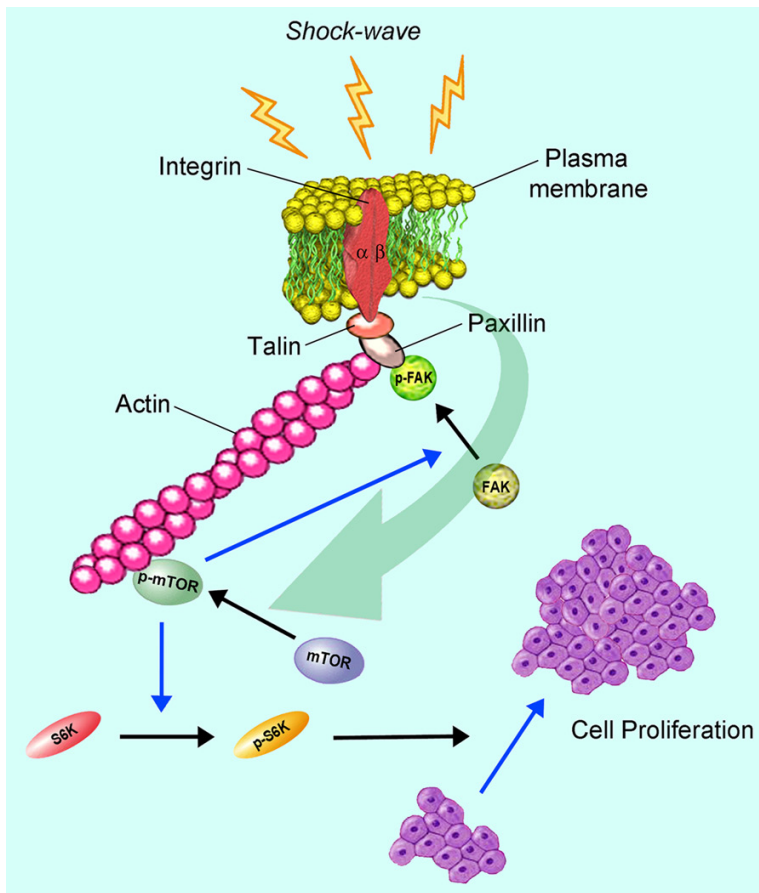


Figure 9. Remodeling of FA complex in response to SW-elicited mechanical force. SW-induced mechanotransduction (green arrow) triggers p-mTOR. The p-mTOR then becomes associated with F-actin. Not only does p-mTOR mediate the phosphorylation of FAK leading to its translocation to FA, but it also phosphorylates ribosomal protein S6 kinase (S6K, an mTOR readout protein) causing cell proliferation.

of blood pressure on cardiomyocytes, thereby activating GSK-3 β , Akt, and mTORC1, and (2) GSK-3 β , Akt, and mTORC1 are upstream kinases governing FAK Y576/Y577 phosphorylation. After pre-treatment of MSC with lithium chloride (GSK-3 β inhibitor), LY294002 (PI3K-Akt signaling inhibitor), or rapamycin (mTORC1 inhibitor) for 12 hours, 2 hours, 12 hours, respectively, before delivery of SW of EFD 0.12 mJ/mm², Western blot analysis showed that rapamycin treatment effectively abolishes FAK phosphorylation, while lithium chloride treatment partially reduces and LY294002 administration has no notable effect on FAK phosphorylation following SW stimulation. The results, therefore, indicate that mTORC1, but not GSK-3 β or Akt, is an upstream kinase for SW-elicited FAK phosphorylation (**Figure 6A**).

SW induces mTORC1 phosphorylation as reflected in S6K phosphorylation

After SW application, the MSC were harvested at 12 h post-SW and the cells lysate was subjected to polyacrylamide gradient gel electrophoresis for Western blot analysis. The Western blots from three independent experiments were statistically analyzed to compare the stoichiometric ratio of phosphorylated mTORC1 to non-phosphorylated mTORC1 (**Figure 6B, 6C**). To further confirm the involvement of mTORC1 signalling, the mTORC1 activation readout protein S6K was also examined by Western blot analysis (**Figure 6B, 6D**). The results showed that, unlike the SW-induced FAK phosphorylation that peaks at 0.12 mJ/mm², the p-mTORC1/mTORC1 ratio progressively increases on applying SW of increasing energies from 0 to 0.15 mJ/mm² to MSC despite the above finding of microfilamentous and microtubular destruction when subjected to SW of EFD over 0.13 mJ/mm². The result implies that mTORC1 phosphorylation is not affected by structural integrity of microfilaments or microtubules.

phorylation is not affected by structural integrity of microfilaments or microtubules.

Rapamycin abolishes SW-induced FAK activation and subsequent paxillin phosphorylation

To confirm the role of mTOR in regulating FAK phosphorylation, prior to SW application, the MSC were treated with or without rapamycin. SW of EFD ranging from 0.1 to 0.15 mJ/mm² was applied to MSC that were harvested 12 hours later for Western blot analysis. The results were consistent with those from former experiments that SW of energy 0.12 mJ/mm² induced maximal FAK phosphorylation and kinase activity but the capacity was abolished after rapamycin treatment (**Figure 6E**). To examine the enzymatic activity of p-FAK, the Western blotted membranes were probed with

antibody against p-Y31 paxillin. Similarly, paxillin was found to be phosphorylated at tyrosine 31 in MSC treated with SW of energy 0.12 mJ/mm², but phosphorylation of FAK is abrogated in the rapamycin-pretreated MSC. This result indicates that paxillin phosphorylation is dependent on the SW-activated catalytic function of mTOR and FAK (**Figure 6E**).

Co-ordinated regulation of FAK activation by mTORC1 and microfilaments

Immunofluorescent staining showed that mTOR was distributed in a punctuated pattern dispersed in the cytoplasm without SW treatment (**Figure 7A**), whereas mTOR was assembled in vesicle-like inclusions associated with the actin stress fibers after SW treatment. The finding suggests that SW induces a subcellular translocation of mTOR.

On the other hand, mTOR exhibited a punctuated pattern associated with actin stress fibers after rapamycin pretreatment before SW application instead of vesicle-like inclusions, while mTOR granules lost its association with actin stress fibers in cells pretreated with cytochalasin D before SW stimulation (**Figure 7A**). The results, therefore, indicate a co-ordinated regulation of FAK phosphorylation by mTORC1 and microfilaments, which are important for the formation of vesicle-like mTOR inclusions and their association with microfilaments, respectively.

To study the roles of actin stress fibers and mTORC1 in FAK subcellular localization, the cells were also stained with antibody against FAK and TRITC-tagged phalloidin after being pretreated with rapamycin and cytochalasin D, respectively, before SW application (**Figure 7B**). The results indicated neither FAK translocation nor its association with actin stress fibers after pretreatment with rapamycin (an mTORC1 inhibitor) or cytochalasin D (CD, an actin depolymerizing factor) before SW stimulation. Accordingly, the findings indicated a combined regulation of actin stress fiber and mTORC1 in SW-induced FAK activation and translocation to focal adhesions.

SW activates mTORC1 signaling for cell proliferation

To verify the significance of mTORC1 and mTORC1-FAK signaling axis in MSC prolifera-

tion, MSC were cultured with FAK pre-depleted by siRNA and mTORC1 inhibited by rapamycin in serum-free conditions to abolish the effects of serum or potential nutrients/growth factors on mTORC1 phosphorylation before SW treatment at an EFD of 0.12 mJ/mm².

At post-SW 24 h, 48 h, 72 h and 96 h, exponential multiplication was noted in the cultured cells without FAK siRNA or rapamycin treatment in serum-free medium with a growth rate comparable to that of cells cultured in medium containing 10% FBS (**Figure 8**). At the other end of the spectrum, cells pretreated with rapamycin exhibited the poorest growth despite SW treatment. On the other hand, cells with FAK depletion before SW treatment and those cultured in serum-free medium showed significantly suppressed cell growth compared to cells receiving pure SW treatment and those cultured in 10% FBS. The results indicate that SW-based MTD activates the mTORC1-FAK axis for promoting cell proliferation.

Discussion

Since FAK phosphorylation has been reported to represent SW-elicited MTD in different cell types [25, 31, 43, 44], the p-FAK/FAK ratio can theoretically identify the upstream regulators of FAK phosphorylation. Our results suggest that microfilament is an essential cellular component mediating SW-stimulated FAK phosphorylation at Y576 and Y577, and that SW of EFD above 0.13 mJ/mm² results in collapse of microfilaments and deregulation of FAK phosphorylation independent of mTOR activation. In addition to biomechanics, the microfilaments can withstand SW energy of 0.12 mJ/mm² which is also the optimal energy level for promoting FAK phosphorylation.

In our model, the net energy directly acting on the plasma membrane of MSC was actually lower than 0.12 mJ/mm², after taking into account the plastic cover and thickness of buffer. In this way, our results identified SW energy of 0.12 mJ/mm² as an optimal level for FAK phosphorylation and that an energy level above 0.13 mJ/mm² is detrimental to cytoskeleton. Our result is supported by the finding of another study that demonstrated a level between 0.10 mJ/mm² and 0.13 mJ/mm² as the optimal energy for minimizing apoptosis in rat bone marrow-derived endothelial progenitor cells [45].

Microfilament is an essential component mediating SW-triggered FAK phosphorylation

The results of the present study demonstrated that both mechanical destruction and chemical depolymerization of cytoskeleton can interrupt SW-induced FAK phosphorylation in MSC, highlighting the pivotal role of microfilaments in SW-based MTD in the FAK signalling axis. Consistently, it has previously been shown that a pulling force on integrin causes FAK activation in neuronal cells [14]. In that study, a traction force of >60pN applied on integrin of extending axon results in FAK phosphorylation at Y396, Y576 and Y577, suggesting that actin filaments and actomyosin contraction are mediators of MTD for FAK phosphorylation [14]. In support of our hypothesis that SW can trigger FAK phosphorylation by mechanical transduction through microfilaments, the results of the present study demonstrated that chemical depolymerization and mechanical destruction of microfilaments by high-energy SW disrupt FAK phosphorylation. On the other hand, consistent with the finding of a previous study showing an important role of microtubules in disassembling of FAK-associated focal adhesions [46], colchicine-induced depolymerization of microtubules in the current study causes a significant upregulation of FAK phosphorylation and increase in size of focal adhesions (**Figure 5A-D**).

Shock-wave induces mTORC1 phosphorylation

In the present study, SW intensity-dependent phosphorylation of mTORC1 supports the role of mTOR as a pressure-sensing protein. Besides, progressive phosphorylation beyond an energy level of 0.13 mJ/mm² at which the microfilaments and microtubules were disrupted also indicates that mTOR phosphorylation is independent of the integrity of cytoskeleton because of its nature as a membrane-associated protein [47]. However, SW does affect subcellular localization of mTOR in our experimental model. The proposal of SW-induced activation of mTOR is rational with the knowledge that both subcellular localization of mTOR and mTOR phosphorylation are prerequisites for its biological activity [48, 49].

Coordinated regulation of FAK activation by actin cytoskeleton and mTORC1 and its translocation to focal adhesions

Although subcellular localization of mTOR has been demonstrated to be critical for the activa-

tion of its downstream effectors and allocation to different subcellular compartments in response to different forms of stress [37, 48, 49], the role of actin in regulating mTOR dynamics and the effect of altered localization of organelles (e.g., lysosomes) on mTORC1 activity remain unclear [48]. In the present study, we found that SW, which is an external mechanical stress, causes subcellular translocations of mTOR as vesicle-like inclusions associated with actin stress fiber on reacting with antibody against mTOR and TRITC-phalloidin against microfilament (**Figure 7B**). Since physical destruction of F-actin with high-energy SW and chemical inactivation of mTORC1 with rapamycin are able to interrupt the assembling of the vesicle-like inclusions or their association with the actin stress fibers (**Figure 7A**), our results showed, for the first time, that the phosphorylation of FAK and its subcellular translocation to focal adhesions require the co-ordination of mTORC1 activation and microfilament remodeling. Taken together, based on immunofluorescent observation and Western blot analysis, we demonstrated that SW-induced FAK activation involves a coordinated regulation by actin filaments and phosphorylated mTORC1 (**Figures 6B, 6E, 7B**).

mTORC1-FAK signaling axis

The principal finding of the present study is that TORC1 activates FAK through phosphorylation at Y576/Y577 with its translocation to focal adhesions (**Figure 6A-E**). mTORC1-mediated FAK phosphorylation and translocation to focal adhesion has been reported in tumor cells by type I insulin-like growth factor (IGF) stimulation [50]. Here we report the mTORC1-FAK signaling axis as a novel signaling pathway of MTD in MSC.

Hornberger and other investigator demonstrated that mTORC1 and FAK are mechanosensing proteins involved in cell proliferation in an *in vivo* study of skeletal muscle stretching [33, 37, 51, 52]. That study showed that MTD from stretching activates mTORC1 and FAK in an Akt signaling-independent fashion [33, 37]. The finding is in concert with that of the current study in which inhibition of PI3-Akt signaling by LY294002 does not negatively affect SW-induced mTORC1 and FAK phosphorylation (**Figure 6A**). Additionally, we further demonstrated that mTOR regulates phosphorylation of FAK as reflected in an increase in size of focal adhesions (**Figures 6E, 7B**).

A previous study showed that FAK over-expression in transgenic mice resulted in cardiac hypertrophy that was significantly alleviated after rapamycin treatment, highlighting a unique role of FAK in regulating the signaling mechanisms governing myocyte growth [34, 53, 54]. Although the authors suggest that FAK activation may control the activity of p13K/AKT/mTOR pathway and could be important for the adaptive response to increase in cardiac afterload, the upstream regulator was not characterized [40, 55, 56]. Importantly, our results revealed that FAK activation is regulated by mTOR, which acts as the upstream regulator instead of PI3K and AKT. The present study is the first to disclose the significance of the mTOR-FAK axis in MTD -elicited modification of focal adhesion maturation. The finding, therefore, may warrant further study in the hypertension setting. Of particular importance was that mTOR activation after SW application was the first report by our present study. Accordingly, the present study is the first to delineate the molecular-cellular signal pathway underlying the effect of shock-wave on focal adhesion complex. The proposed mechanism based on our findings is schematically illustrated in **Figure 9**.

In conclusion, the present study not only demonstrated an essential co-ordinated regulatory pathway of FAK phosphorylation by mTORC1 and microfilaments, but also identified the participation of mTORC1-FAK signalling in MSC proliferation.

Acknowledgements

The study was supported by a grant from Chang Gung Memorial Hospital, Chang Gung University (Grant number: CMRPG8B1361, CMRPG8B13-62 and CMRPG8B1363).

Disclosure of conflict of interest

None.

Authors' contribution

CMY, RF, YTC, JJS, YLC, and CJW conducted experiments and analyzed the data. FYL, YYZ, CKS, and HKY conceived the study, analyzed, and interpreted the data and wrote the manuscript.

Address correspondence to: Dr. Cheuk-Kwan Sun, Department of Emergency Medicine, E-Da Hospital, I-Shou University School of Medicine for International Students, No. 1, Yi-Da Road, Jiao-Su Village, Yan-Chao District, Kaohsiung 82445, Taiwan. Tel: +886 975106203; Fax: +886 7 6150915; E-mail: lawrence.c.k.sun@gmail.com; Hon-Kan Yip, Division of Cardiology, Department of Internal Medicine, Kaohsiung Chang Gung Memorial Hospital and Chang Gung University College of Medicine, 123 Ta-Pei Road, Niao-Sung District, Kaohsiung 83301, Taiwan. Tel: +886 7 7317123 Ext. 8300; Fax: +886 7 7322402; E-mail: han.gung@msa.hinet.net

References

- [1] Copland IB, Reynaud D, Pace-Asciak C and Post M. Mechanotransduction of stretch-induced prostanoid release by fetal lung epithelial cells. *Am J Physiol Lung Cell Mol Physiol* 2006; 291: L487-495.
- [2] Ingber DE. Mechanobiology and diseases of mechanotransduction. *Ann Med* 2003; 35: 564-577.
- [3] DuFort CC, Paszek MJ and Weaver VM. Balancing forces: architectural control of mechanotransduction. *Nat Rev Mol Cell Biol* 2011; 12: 308-319.
- [4] Orr AW, Helmke BP, Blackman BR and Schwartz MA. Mechanisms of mechanotransduction. *Dev Cell* 2006; 10: 11-20.
- [5] Kuo JC. Mechanotransduction at focal adhesions: integrating cytoskeletal mechanics in migrating cells. *J Cell Mol Med* 2013; 17: 704-712.
- [6] Nadruz W Jr, Corat MA, Marin TM, Guimaraes Pereira GA and Franchini KG. Focal adhesion kinase mediates MEF2 and c-Jun activation by stretch: role in the activation of the cardiac hypertrophic genetic program. *Cardiovasc Res* 2005; 68: 87-97.
- [7] Zhou D, Herrick DJ, Rosenbloom J and Chaqour B. Cyr61 mediates the expression of VEGF, alphav-integrin, and alpha-actin genes through cytoskeletally based mechanotransduction mechanisms in bladder smooth muscle cells. *J Appl Physiol* (1985) 2005; 98: 2344-2354.
- [8] Anwar MA, Shalhoub J, Lim CS, Gohel MS and Davies AH. The effect of pressure-induced mechanical stretch on vascular wall differential gene expression. *J Vasc Res* 2012; 49: 463-478.
- [9] Colombelli J, Besser A, Kress H, Reynaud EG, Girard P, Caussinus E, Haselmann U, Small JV, Schwarz US and Stelzer EH. Mechanosensing in actin stress fibers revealed by a close correlation between force and protein localization. *J Cell Sci* 2009; 122: 1665-1679.

mTOR-FAK axis and cell proliferation

- [10] Hoffman BD, Grashoff C and Schwartz MA. Dynamic molecular processes mediate cellular mechanotransduction. *Nature* 2011; 475: 316-323.
- [11] Arnoczky SP, Tian T, Lavagnino M and Gardner K. Ex vivo static tensile loading inhibits MMP-1 expression in rat tail tendon cells through a cytoskeletonally based mechanotransduction mechanism. *J Orthop Res* 2004; 22: 328-333.
- [12] Balasubramanian L, Ahmed A, Lo CM, Sham JS and Yip KP. Integrin-mediated mechanotransduction in renal vascular smooth muscle cells: activation of calcium sparks. *Am J Physiol Regul Integr Comp Physiol* 2007; 293: R1586-1594.
- [13] Beurg M, Nam JH, Chen Q and Fettilplace R. Calcium balance and mechanotransduction in rat cochlear hair cells. *J Neurophysiol* 2010; 104: 18-34.
- [14] Moore SW, Zhang X, Lynch CD and Sheetz MP. Netrin-1 attracts axons through FAK-dependent mechanotransduction. *J Neurosci* 2012; 32: 11574-11585.
- [15] Oakes PW and Gardel ML. Stressing the limits of focal adhesion mechanosensitivity. *Curr Opin Cell Biol* 2014; 30: 68-73.
- [16] Papisheva E and Heisenberg CP. Spatial organization of adhesion: force-dependent regulation and function in tissue morphogenesis. *EMBO J* 2010; 29: 2753-2768.
- [17] Lim Y, Lim ST, Tomar A, Gardel M, Bernard-Trifilo JA, Chen XL, Uryu SA, Canete-Soler R, Zhai J, Lin H, Schlaepfer WW, Nalbant P, Bokoch G, Ilic D, Waterman-Storer C and Schlaepfer DD. PyK2 and FAK connections to p190Rho guanine nucleotide exchange factor regulate RhoA activity, focal adhesion formation, and cell motility. *J Cell Biol* 2008; 180: 187-203.
- [18] Brown MC, Cary LA, Jamieson JS, Cooper JA and Turner CE. Src and FAK kinases cooperate to phosphorylate paxillin kinase linker, stimulate its focal adhesion localization, and regulate cell spreading and protrusiveness. *Mol Biol Cell* 2005; 16: 4316-4328.
- [19] Calalb MB, Polte TR and Hanks SK. Tyrosine phosphorylation of focal adhesion kinase at sites in the catalytic domain regulates kinase activity: a role for Src family kinases. *Mol Cell Biol* 1995; 15: 954-963.
- [20] Zebda N, Dubrovskiy O and Birukov KG. Focal adhesion kinase regulation of mechanotransduction and its impact on endothelial cell functions. *Microvasc Res* 2012; 83: 71-81.
- [21] Brami-Cherrier K, Gervasi N, Arsenieva D, Walkiewicz K, Bouterin MC, Ortega A, Leonard PG, Seantier B, Gasmi L, Bouceba T, Kadare G, Girault JA and Arold ST. FAK dimerization controls its kinase-dependent functions at focal adhesions. *EMBO J* 2014; 33: 356-370.
- [22] Hanks SK, Ryzhova L, Shin NY and Brabek J. Focal adhesion kinase signaling activities and their implications in the control of cell survival and motility. *Front Biosci* 2003; 8: d982-996.
- [23] Skalski M, Sharma N, Williams K, Kruspe A and Coppelino MG. SNARE-mediated membrane traffic is required for focal adhesion kinase signaling and Src-regulated focal adhesion turnover. *Biochim Biophys Acta* 2011; 1813: 148-158.
- [24] Peshkovsky SL and Peshkovsky AS. Shockwave model of acoustic cavitation. *Ultrason Sonochem* 2008; 15: 618-628.
- [25] Sun CK, Shao PL, Wang CJ and Yip HK. Study of vascular injuries using endothelial denudation model and the therapeutic application of shock wave: a review. *Am J Transl Res* 2011; 3: 259-268.
- [26] Craig DH, Haimovich B and Basson MD. Alpha-actinin-1 phosphorylation modulates pressure-induced colon cancer cell adhesion through regulation of focal adhesion kinase-Src interaction. *Am J Physiol Cell Physiol* 2007; 293: C1862-1874.
- [27] Olsen SM, Stover JD and Nagatomi J. Examining the role of mechanosensitive ion channels in pressure mechanotransduction in rat bladder urothelial cells. *Ann Biomed Eng* 2011; 39: 688-697.
- [28] Shim JW, Wise DA and Elder SH. Effect of Cytoskeletal Disruption on Mechanotransduction of Hydrostatic Pressure by C3H10T1/2 Murine Fibroblasts. *Open Orthop J* 2008; 2: 155-162.
- [29] Hofmann A, Ritz U, Hessmann MH, Alini M, Rommens PM and Rompe JD. Extracorporeal shock wave-mediated changes in proliferation, differentiation, and gene expression of human osteoblasts. *J Trauma* 2008; 65: 1402-1410.
- [30] Kearney CJ, Lee JY, Padera RF, Hsu HP and Spector M. Extracorporeal shock wave-induced proliferation of periosteal cells. *J Orthop Res* 2011; 29: 1536-1543.
- [31] Xu JK, Chen HJ, Li XD, Huang ZL, Xu H, Yang HL and Hu J. Optimal intensity shock wave promotes the adhesion and migration of rat osteoblasts via integrin beta1-mediated expression of phosphorylated focal adhesion kinase. *J Biol Chem* 2012; 287: 26200-26212.
- [32] Bodine SC, Stitt TN, Gonzalez M, Kline WO, Stover GL, Bauerlein R, Zlotchenko E, Scrimgeour A, Lawrence JC, Glass DJ and Yancopoulos GD. Akt/mTOR pathway is a crucial regulator of skeletal muscle hypertrophy and can prevent muscle atrophy in vivo. *Nat Cell Biol* 2001; 3: 1014-1019.
- [33] Hornberger TA, Stuppard R, Conley KE, Fedele MJ, Fiorotto ML, Chin ER and Esser KA. Mechanical stimuli regulate rapamycin-sensitive signalling by a phosphoinositide 3-kinase, pro-

- tein kinase B- and growth factor-independent mechanism. *Biochem J* 2004; 380: 795-804.
- [34] Houssaini A, Abid S, Mouraret N, Wan F, Rideau D, Saker M, Marcos E, Tissot CM, Dubois-Rande JL, Amsellem V and Adnot S. Rapamycin reverses pulmonary artery smooth muscle cell proliferation in pulmonary hypertension. *Am J Respir Cell Mol Biol* 2013; 48: 568-577.
- [35] Lee RT and Huang H. Mechanotransduction and arterial smooth muscle cells: new insight into hypertension and atherosclerosis. *Ann Med* 2000; 32: 233-235.
- [36] Mejias M, Garcia-Pras E, Gallego J, Mendez R, Bosch J and Fernandez M. Relevance of the mTOR signaling pathway in the pathophysiology of splenomegaly in rats with chronic portal hypertension. *J Hepatol* 2010; 52: 529-539.
- [37] Philp A, Hamilton DL and Baar K. Signals mediating skeletal muscle remodeling by resistance exercise: PI3-kinase independent activation of mTORC1. *J Appl Physiol* (1985) 2011; 110: 561-568.
- [38] Rice KM, Kinnard RS, Wright GL and Blough ER. Aging alters vascular mechanotransduction: pressure-induced regulation of p70S6k in the rat aorta. *Mech Ageing Dev* 2005; 126: 1213-1222.
- [39] Proud CG. Ras, PI3-kinase and mTOR signaling in cardiac hypertrophy. *Cardiovasc Res* 2004; 63: 403-413.
- [40] Sugimura K, Fukumoto Y, Nawata J, Wang H, Onoue N, Tada T, Shirato K and Shimokawa H. Hypertension promotes phosphorylation of focal adhesion kinase and proline-rich tyrosine kinase 2 in rats: implication for the pathogenesis of hypertensive vascular disease. *Tohoku J Exp Med* 2010; 222: 201-210.
- [41] Chao JT and Davis MJ. The roles of integrins in mediating the effects of mechanical force and growth factors on blood vessels in hypertension. *Curr Hypertens Rep* 2011; 13: 421-429.
- [42] Koller A. Signaling pathways of mechanotransduction in arteriolar endothelium and smooth muscle cells in hypertension. *Microcirculation* 2002; 9: 277-294.
- [43] Yu T, Junger WG, Yuan C, Jin A, Zhao Y, Zheng X, Zeng Y and Liu J. Shockwaves increase T-cell proliferation and IL-2 expression through ATP release, P2X7 receptors, and FAK activation. *Am J Physiol Cell Physiol* 2010; 298: C457-464.
- [44] Wang CJ. An overview of shock wave therapy in musculoskeletal disorders. *Chang Gung Med J* 2003; 26: 220-232.
- [45] Zhang X, Yan X, Wang C, Tang T and Chai Y. The dose-effect relationship in extracorporeal shock wave therapy: the optimal parameter for extracorporeal shock wave therapy. *J Surg Res* 2014; 186: 484-492.
- [46] Ezratty EJ, Partridge MA and Gundersen GG. Microtubule-induced focal adhesion disassembly is mediated by dynamin and focal adhesion kinase. *Nat Cell Biol* 2005; 7: 581-590.
- [47] Liu X and Zheng XF. Endoplasmic reticulum and Golgi localization sequences for mammalian target of rapamycin. *Mol Biol Cell* 2007; 18: 1073-1082.
- [48] Betz C and Hall MN. Where is mTOR and what is it doing there? *J Cell Biol* 2013; 203: 563-574.
- [49] Partovian C, Ju R, Zhuang ZW, Martin KA and Simons M. Syndecan-4 regulates subcellular localization of mTOR Complex2 and Akt activation in a PKC α -dependent manner in endothelial cells. *Mol Cell* 2008; 32: 140-149.
- [50] Liu L, Chen L, Chung J and Huang S. Rapamycin inhibits F-actin reorganization and phosphorylation of focal adhesion proteins. *Oncogene* 2008; 27: 4998-5010.
- [51] Gordon SE, Fluck M and Booth FW. Selected Contribution: Skeletal muscle focal adhesion kinase, paxillin, and serum response factor are loading dependent. *J Appl Physiol* (1985) 2001; 90: 1174-1183; discussion 1165.
- [52] Hornberger TA. Mechanotransduction and the regulation of mTORC1 signaling in skeletal muscle. *Int J Biochem Cell Biol* 2011; 43: 1267-1276.
- [53] Clemente CF, Xavier-Neto J, Dalla Costa AP, Consonni SR, Antunes JE, Rocco SA, Pereira MB, Judice CC, Strauss B, Joazeiro PP, Matos-Souza JR and Franchini KG. Focal adhesion kinase governs cardiac concentric hypertrophic growth by activating the AKT and mTOR pathways. *J Mol Cell Cardiol* 2012; 52: 493-501.
- [54] Teo BK, Wong ST, Lim CK, Kung TY, Yap CH, Ramagopal Y, Romer LH and Yim EK. Nanotopography modulates mechanotransduction of stem cells and induces differentiation through focal adhesion kinase. *ACS Nano* 2013; 7: 4785-4798.
- [55] Hsieh HJ, Liu CA, Huang B, Tseng AH and Wang DL. Shear-induced endothelial mechanotransduction: the interplay between reactive oxygen species (ROS) and nitric oxide (NO) and the pathophysiological implications. *J Biomed Sci* 2014; 21: 3.
- [56] Knoll R, Hoshijima M, Hoffman HM, Person V, Lorenzen-Schmidt I, Bang ML, Hayashi T, Shiga N, Yasukawa H, Schaper W, McKenna W, Yokoyama M, Schork NJ, Omens JH, McCulloch AD, Kimura A, Gregorio CC, Poller W, Schaper J, Schultheiss HP and Chien KR. The cardiac mechanical stretch sensor machinery involves a Z disc complex that is defective in a subset of human dilated cardiomyopathy. *Cell* 2002; 111: 943-955.
- [57] Sasoh A, Ohtani T and Mori K. Pressure effect in a shock-wave-plasma interaction induced by a focused laser pulse. *Phys Rev Lett* 2006; 97: 205004.

Supplemental materials and methods

Isolation of adipose tissue from SD rat, MSC preparation and culture

The use of 10 male SD rats, age 8-12 weeks, this protocol was approved by the Institutional Animal Care and Use Committee (IACUC) of Kaohsiung Chang Gung Memorial Hospital (number: AN-201312809). In brief, Rats are under general anaesthesia with 2-3% isoflurane. The rats were maintained under anaesthesia (a mixture of isoflurane (3.5 L/min) and 100% oxygen (3 L/min)) throughout the surgical procedure. Facilities are temperature-controlled (23°C to 25°C), and rats were restrained on heating pads in a standardized fashion to maintain their body temperature at 37°C. The ventral area was shaved and swabbed with surgical scrub, iodine and alcohol. Upward 3 cm from base of tail, a 2-3 cm ventral midline skin incision was made. A single incision of 1-2 cm long was made into the muscle wall. The adipose tissue in scrotal region was exteriorized. Under laminar hood, the specimen was minced into small pieces and then subjected to enzymatic digestion with the ratio 1 g adipose tissue to 1 mL collagenase type II (0.2 mg/mL) in HBSS at 37°C for 30 minutes. After digestion, the adipose tissue was homogenized with 200 µm strainer. The floating cells were separated from the remnant fatty tissue by centrifugation (200 G) for 5 min. The pellet (stromal cell fraction) was then filtered through a 200 µm strainer to remove undigested tissue. The cells were suspended in 1 mL culture medium, including DMEM with 1500 mg/mL glucose (Dulbecco Modified Eagle Medium, Gibco, USA) supplemented with 10% FBS (fetal bovine serum, Gibco, USA) and 10 IU/mL penicillin/streptomycin (Gibco, UAS) and plated at 5×10^5 cells/mL in a 100 mm Petri dish. The cells were incubated in an atmosphere of 5% CO₂ at 37°C. Twelve hours later, the suspending cells were removed. The adherent cells were washed in PBS twice. The cells were fed in fresh DMEM supplemented with 10% FBS and 10 IU/mL penicillin/streptomycin. Two days after culture initiation, the medium was discarded and the cells were fed with fresh medium. Medium changes were performed every 2 days until the cells density became confluent. Then the cells were trypsinized using 0.05% trypsin/1 mM EDTA and passaged at 1:3 ratios into new 100 mm Petri dishes. Subculture was repeated until passage 3 when sufficient cells were provided for the next stage of experiment. MSC between passage 3 and passage 8 were applied this study.

Protein extraction and immunoblot

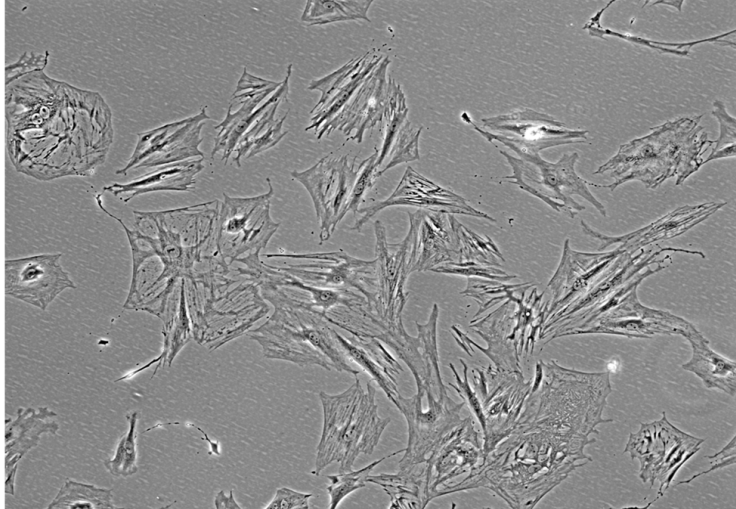
Cells were harvested after 12 hours shock-wave application. Cells were lysed in Ripa buffer (Sigma-Aldrich), and the cell lysate was passed 10 times through an 18 G needle to homogenate cells. Protein concentration was determined using bicinchoninic acid procedure (Pierce Biochemical company). Then 30 µg of proteins from cells lysate were resolved on 8 or 10% SDS-poly-acrylamide gel. To detect mTORC1 and p-mTOR, the 30 µg of proteins were resolved on 6-20% gradient SDS-poly-acrylamide gel. After protein migration, the proteins were blotted on PVDF membrane (Immobilon 0.45 m, Millipore). The membranes were blocked in 5% silk milk for 2 h in TBST buffer (20 mM Tris-Cl, 150 mM NaCl, 0.1% Tween 20, pH 7.4). For antibody probing, membranes were incubated with first antibody for 2 h. Immuno-reactive signals were detected by incubation with horseradish peroxidase conjugated-secondary for 2 h and followed by enhanced chemiluminescent detection using Pierce ECL Western Blotting Substrate (Thermo Scientific). The immunoblot imaging was captured by using BioSpectrum AC Imaging System (Ultra-Violet Product Ltd.). The protein bands were quantified using ImageQuant software (GE-Healthcare) and digitally converted relative value for statistical analysis.

Cell proliferation assay

Cell proliferation assay was carried out by cell number calculation. The 10^5 cells were seeded in a well of 6 wells-plate and cultured in serum free DMEM. After 24 h, 48 h, 72 h and 96 h culture, cells were trypsinized and stained with 0.4% typhan blue (Sigma). The unstained cells were counted by using hemocytometer. The proliferative index was calculated as the number of cells from three independent experiments. The five distinct groups were settled in this proliferation assay. The shock-wave treated cells were treated with shock-wave 0.12 mJ/mm², 100 pluses. The cells with pharmacological mTORC1 inhibition were treated 5 µM rapamycin for 2 h prior to shock-wave application. The 10^6 cells that were depleted with FAK were performed siFAK oligonucleotides transfection for 24 h were treated with shock-wave. After shock-wave application, cells were counted and 10^5 cells were reseeded in a 35 mm Petri dish for cells proliferation assay.

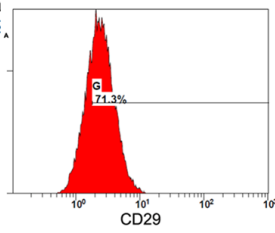
mTOR-FAK axis and cell proliferation

A

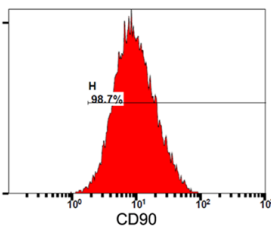


Supplementary Figure 1. A. The fibroblast-like morphology in cultured mesenchymal stem cells. B. Flow cytometric analysis of mesenchymal stem cells (MSC). C. Schematic representation of the shock-wave treatment model.

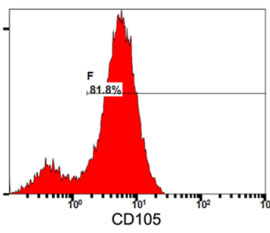
B a



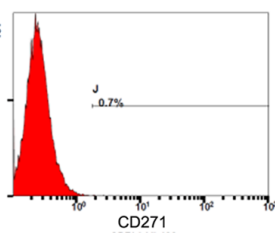
b



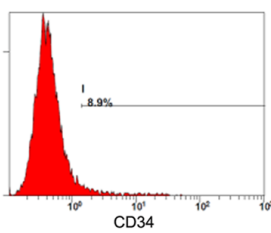
c



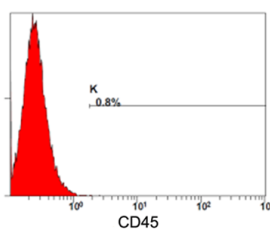
d



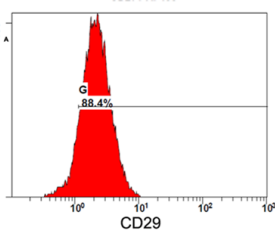
e



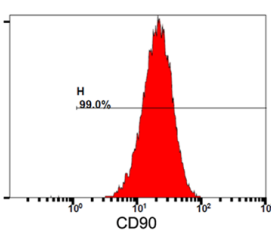
f



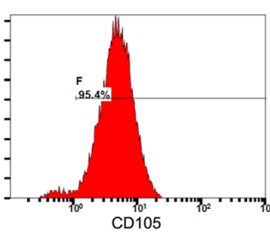
g



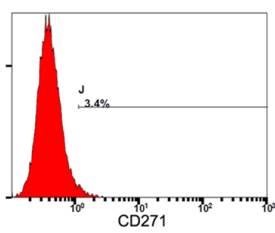
h



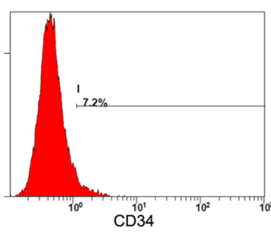
i



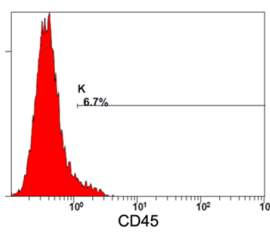
j



k



l



C

